Acta Cryst E CRYSTALLOGRAPHIC COMMUNICATIONS

ISSN 2056-9890

Crystal structure and Hirshfeld surface analysis of 4-bromo-6-phenyl-6,7-dihydro-5*H*-furo[2,3-*f*]-isoindol-5-one

Kseniia A. Alekseeva,[a] Mikhail S. Grigoriev,[b] Irina A. Kolesnik,[c] Narmin A. Murshudlu,[d] Khudayar I. Hasanov,[e] Roya Z. Nazarova,[f] Mehmet Akkurt[g] and Gizachew Mulugeta Manahelohe[h]*

[a]RUDN University, 6 Miklukho-Maklaya St., Moscow 117198, Russian Federation, [b]Frumkin Institute of Physical Chemistry and Electrochemistry, Russian Academy of Sciences, Leninsky prosp. 31, bld. 4, 119071, Moscow, Russian Federation, [c]Institute of Physical Organic Chemistry, National Academy of Sciences of Belarus, 220072 Minsk, Belarus, [d]Department of Chemistry, Faculty of Natural Sciences, Sumgait State University, Baku Str. 1, AZ 5008, Sumgait, Azerbaijan, [e]Azerbaijan Medical University, Scientific Research Centre (SRC), A. Kasumzade St. 14, AZ 1022, Baku, Azerbaijan, [f]Baku Engineering University, Khirdalan, Hasan Aliyev str. 120, AZ0101, Absheron, Azerbaijan, [g]Department of Physics, Faculty of Sciences, Erciyes University, 38039 Kayseri, Türkiye, and [h]Department of Chemistry, University of Gondar, PO Box 196, Gondar, Ethiopia. *Correspondence e-mail: Gizachew.Mulugeta@uog.edu.et

Received 30 July 2025
Accepted 12 August 2025

Edited by B. Therrien, University of Neuchâtel, Switzerland

Keywords: crystal structure; isoindole; furo[2,3-*f*]isoindole; IMDAV reaction; Diels–Alder reaction; Hirshfeld surface analysis.

CCDC reference: 2479912

Supporting information: this article has supporting information at journals.iucr.org/e

The title molecule, $C_{16}H_{10}BrNO_2$, is essentially planar (r.m.s. deviation = 0.004 Å). In the crystal, molecules are linked by C—H···O and C—H···Br hydrogen bonds, forming ribbons along the *b*-axis direction. Furthermore, π-π interactions cause the molecules to form ribbons along the [1 0 $\overline{1}$0] and [1 0 10] directions [centroid-to-centroid distances = 3.703 (3), 3.734 (3), 3.703 (3), and 3.734 (3) Å]. According to a Hirshfeld surface analysis, H···H (33.8%), O···H/H···O (15.1%), C···H/H···C (14.6%), Br···H/H···Br (13.8%), and C···C (11.9%) interactions are the main contributors to the crystal packing.

1. Chemical context

Isoindoles and their partially hydrogenated and/or condensed derivatives are widely occurring heterocycles in nature. This scaffold has significant applications in diverse fields, including medicine, photoactive materials, coordination chemistry, and fine organic synthesis. Their unique structural features allow for the creation of derivatives that exhibit a wide range of biological activities. Consequently, developing novel synthetic methods to overcome existing challenges, as well as reactions that leverage isoindoles to access functionally valuable compounds, has attracted considerable attention (for recent reviews, see: Speck & Magauer, 2013; Weintraub & Wang, 2023; Ou-Ichen *et al.*, 2024).

Over the past decade, our group has explored the construction of fused isoindoles *via* the intramolecular Diels–Alder reaction in vinylarenes (the IMDAV reaction) (Zaytsev *et al.*, 2021, 2023 and a review, Krishna *et al.*, 2022) and expanded its synthetic utility through the development of multicomponent one-pot cascade transformations (Voronov *et al.*, 2018; Alekseeva *et al.*, 2023, 2024). In a recent study (Alekseeva *et al.*, 2020), it was demonstrated that 3-(2-furyl) allylamines and bromomaleic anhydride react *via* an IMDAV reaction followed by dehydrobromination. Furthermore, *in situ*-generated HBr was found to induce an aromaticity transfer from the furan ring to the cyclohexane moiety. Based on this observation, we aimed to investigate whether entirely dehydrogenated fused isoindole could be synthesized directly from 3-arylallylamine and halogen-substituted maleic anhy-

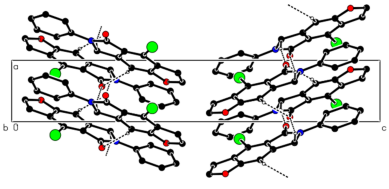

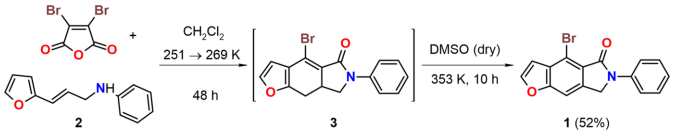

Figure 1
Synthesis of 4-bromo-6-phenyl-6,7-dihydro-5*H*-furo[2,3-*f*]isoindol-5-one.

dride. Given that the IMDAV reaction between 3-(2-furyl) allylamines and maleic anhydride yields 5-oxo-4a,5,6,7,7a,8-hexahydro-4*H*-furo[2,3-*f*]isoindole-4-carboxylic acids (Apponyi *et al.*, 2002; Deng *et al.*, 2019), we hypothesized that employing dibromomaleic anhydride would facilitate the formation of two carbon–carbon double bonds through successive dehydrobromination reactions.

Contrary to our expectations, the reaction between *N*-[(2*E*)-3-(furan-2-yl)prop-2-en-1-yl]aniline (**2**) and dibromomaleic anhydride was accompanied by simultaneous dehydrobromination and decarboxylation. The resulting product (**3**) displayed limited solubility in common deuterated solvents. For its characterization by NMR, compound **3** was dissolved in DMSO-d_6 and heated to 353 K to obtain a clear solution. Surprisingly, NMR analysis indicated that DMSO favours oxidation of **3** to yield 4-bromo-6-phenyl-6,7-dihydro-5*H*-furo[2,3-*f*]isoindol-5-one (**1**) (Fig. 1). This aromatization reaction was subsequently confirmed using non-deuterated DMSO.

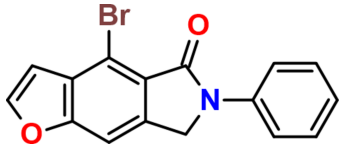

2. Structural commentary

The conformation of the molecule is stabilized by an intramolecular C—H···O hydrogen bond (Table 1, Fig. 2) that forms an *S*(6) motif (Bernstein *et al.*, 1995). Thus, the molecule is planar except for some hydrogen atoms. The distances of the furthest atoms from the least squares plane of the molecule are −0.153 (4), 0.141 (4), −0.097 (4), and 0.090 (5) Å for atoms C15, C12, C16, and C13, respectively. The C5—N6—C11—C12 and C7—N6—C11—C16 torsion angles are 10.9 (6) and 5.7 (5)°, respectively. The geometric parameters of the title compound are normal and consistent with those of related compounds listed in the *Database survey* (Section 4).

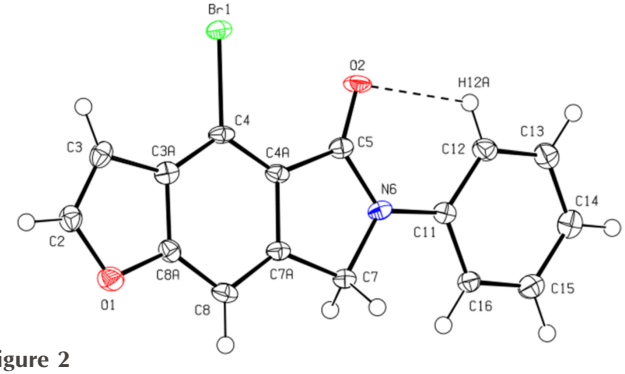

Figure 2
The title molecules showing the atom-labelling scheme with displacement ellipsoids drawn at the 50% probability level.

Table 1
Hydrogen-bond geometry (Å, °).

D—H···*A*	*D*—H	H···*A*	*D*···*A*	*D*—H···*A*
C7—H7*A*···O2^{i}	0.99	2.51	3.463 (5)	162
C8—H8*A*···O2^{ii}	0.95	2.49	3.348 (5)	149
C12—H12*A*···O2	0.95	2.27	2.894 (6)	122
C16—H16*A*···Br1^{ii}	0.95	2.97	3.864 (4)	157

Symmetry codes: (i) $-x+2, y+\frac{1}{2}, -z+\frac{3}{2}$; (ii) $-x+1, y+\frac{1}{2}, -z+\frac{3}{2}$.

3. Supramolecular features

In the crystal, molecules are linked by C—H···O and C—H···Br hydrogen bonds, forming ribbons along the *b*-axis direction (Table 1, Figs. 3 and 4). The molecules are further linked by π–π interactions [$Cg1\cdots Cg3^{i}$ = 3.703 (3) Å, slippage = 1.236 Å; $Cg2\cdots Cg3^{ii}$ = 3.734 (3) Å, slippage = 1.243 Å;

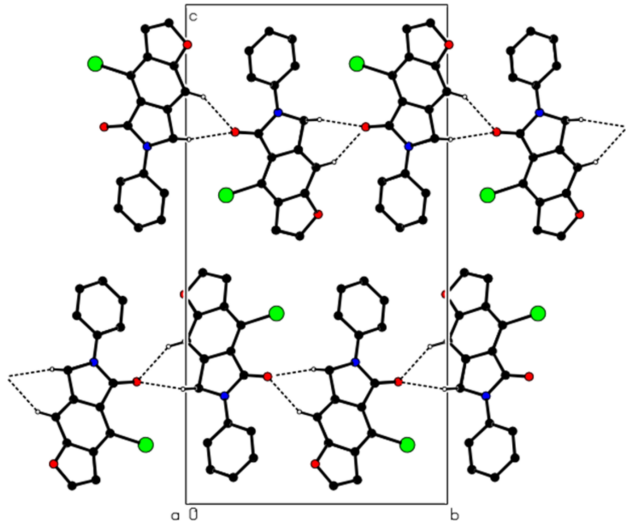

Figure 3
Partial packing of the title compound, viewed down the *a*-axis direction, showing C—H···O and C—H···Br hydrogen bonds as dashed lines. H atoms not involved in these interactions have been omitted for clarity.

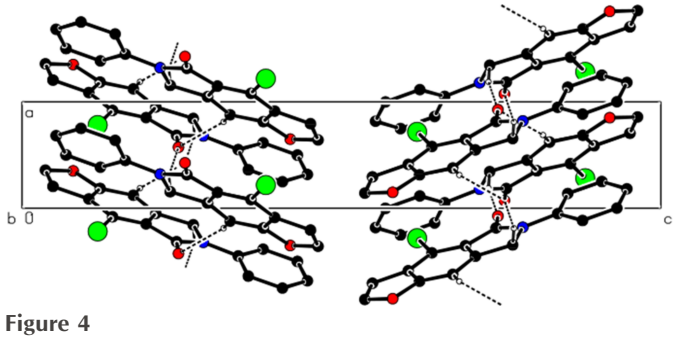

Figure 4
View of the C—H···O and C—H···Br interactions down the *b*-axis direction.

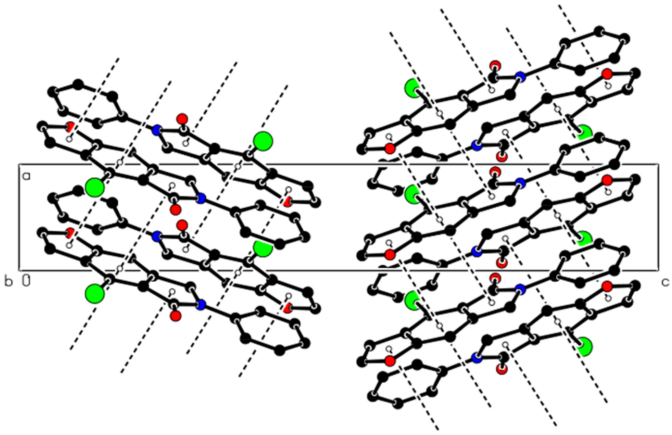

Figure 5
A partial view down the *b*-axis direction showing the π–π interactions (dashed lines).

*Cg*3···*Cg*1^{b} = 3.703 (3) Å, slippage = 1.227 Å; symmetry codes: (i) $-1 + x, y, z$; (ii) $1 + x, y, z$; where *Cg*1, *Cg*2 and *Cg*3 are the centroids of the O1/C2/C3/C3*A*/C8*A*, N6/C5/C4*A*/C7*A*/C7 and C3*A*/C4/C4*A*/C7*A*/C8/C8*A* rings, respectively], thus forming ribbons along the [1 0 $\overline{1}$0] and [1 0 10] directions (Table 1, Fig. 5). C—H···π interactions were not observed.

Using *CrystalExplorer 17.5* (Spackman *et al.*, 2021), a Hirshfeld surface analysis was performed to visualize the intermolecular interactions (Tables 1 and 2). The red and blue areas in the Hirshfeld surface plotted over the d_{norm} (Fig. 6) show contacts that are shorter or longer, respectively, than the van der Waals radii, while the white surface shows contacts with distances equal to the sum of the van der Waals radii

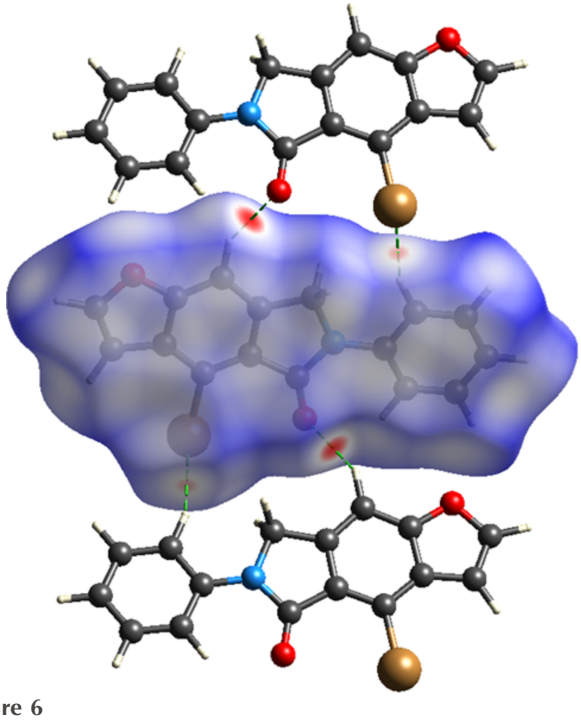

Figure 6
View of the three-dimensional Hirshfeld surface of the title compound plotted over d_{norm}.

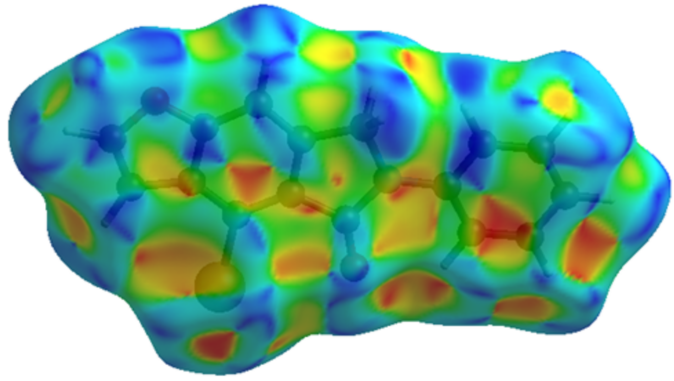

Figure 7
Hirshfeld surface of the title compound plotted over shape-index.

(Venkatesan *et al.*, 2016). Significant π–π interactions are shown by the Hirshfeld surface's shape-index (Fig. 7). Fig. 8 shows the overall two-dimensional fingerprint plot, and Fig. 8*b–f* shows those delineated into H···H (33.8%), O···H/H···O (15.1%), C···H/H···C (14.6%), Br···H/H···Br (13.8%) and C···C (11.9%) interactions. Smaller contributions are made by C···O/O···C (4.9%), C···Br/Br···C

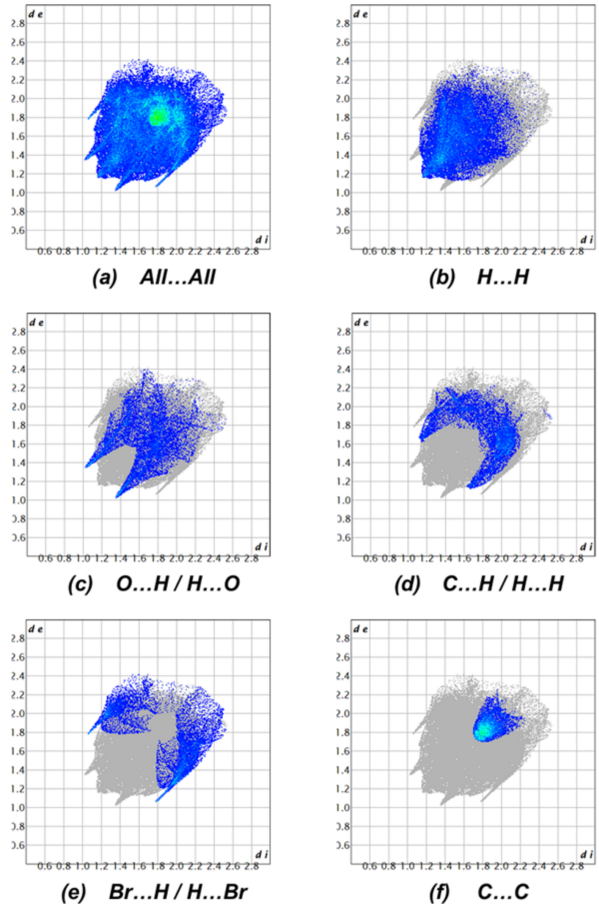

Figure 8
Two-dimensional fingerprint plots, showing (*a*) all interactions, and delineated into (*b*) H···H, (*c*) O···H/H···O, (*d*) C···H/H···C, (*e*) C···Br/Br···C and (*f*) C···C interactions [d_e and d_i represent the distances from a point on the Hirshfeld surface to the nearest atoms outside (external) and inside (internal) the surface, respectively].

Table 2
Short interatomic contacts (Å).

Contact	distance	Symmetry operation
O2···H7*A*	2.51	$2-x, -\frac{1}{2}+y, \frac{3}{2}-z$
O2···H8*A*	2.49	$1-x, -\frac{1}{2}+y, \frac{3}{2}-z$
H7*B*···C11	2.85	$-1+x, y, z$
H2*A*···H15*A*	2.58	$\frac{3}{2}-x, 1-y, -\frac{1}{2}+z$
H3*A*···H3*A*	2.51	$-\frac{1}{2}+x, \frac{1}{2}-y, 1-z$
C14···H14*A*	2.91	$-\frac{1}{2}+x, \frac{1}{2}-y, 2-z$
H2*A*···H15*A*	2.54	$\frac{1}{2}-x, 1-y, -\frac{1}{2}+z$

(2.6%), N···H/H···N (1.8%), C···N/N···C (0.8%), Br···Br (0.6%) and O···O (0.1%) contacts.

4. Database survey

A search of the Cambridge Structural Database (CSD, Version 6.00, last update April 2025; Groom *et al.*, 2016) gave nine hits including the 4-bromo-6-phenyl-6,7-dihydro-5*H*-furo [2,3-*f*]isoindol-5-one unit, five of which were closely related to the title compound, *viz.* CSD refcodes HEMVEE (He *et al.*, 2022), JOGYIP (Zhou *et al.*, 2014), LESXIS (Horak *et al.*, 2013), OJIPUV (Zaytsev *et al.*, 2021) and QADZIH (Zubkov *et al.*, 2016).

π–π and C—H···π interactions are observed in the structure of HEMVEE. In JOGYIP, weak C—H···O interactions lead to the formation of a three-dimensional network and C—H···π interactions are also observed. In LESXIS, O—H···O hydrogen bonds between the carboxylic and carbonyl groups link alternate independent molecules into chains propagating along the *b*-axis direction. The crystal packing also features weak C—H···π interactions. In OJIPUV, molecules are connected by C—H···O hydrogen bonds, C—H···π interactions and π–π stacking interactions, forming a three-dimensional network. In QADZIH, pairs of O—H···O hydrogen bond form dimers with an $R_2^2(8)$ motif. C—H···O hydrogen bonds, π–π and C—H···π interactions were also observed, forming a three-dimensional network.

5. Synthesis and crystallization

N-[(2*E*)-3-(Furan-2-yl)prop-2-en-1-yl]aniline (1.26 mmol) (**2**) was dissolved in dry CH_2Cl_2 (10 mL) and cooled to 251 K. Dibromomaleic anhydride (0.32 g, 1.26 mmol) was added, and the mixture was kept at 269 K for 2 d. The resulting precipitate was filtered, dissolved in dry DMSO (10 mL), and stirred at 353 K for 10 h. The mixture was poured into water (50 mL), the resulting precipitate was filtered off, and washed with water (3 × 3 mL). The product was dried in air to constant weight to afford compound **1** as a light-yellow solid (216.6 mg, 0.66 mmol, 52%), m.p. 481–482 K. A single crystal suitable for X-ray analysis was obtained from DMSO-d_6 upon heating to 353 K and slow cooling to r.t.

^{1}H NMR (700.2 MHz, DMSO-d_6, 333 K) (*J*, Hz): δ 8.21 (*br. d*, *J* = 2.2, 1H, H-2-furyl), 7.90–7.89 (*m*, 3H, H-*ortho*-Ph, H-8), 7.45 (*dd*, *J* = 7.6, 2H, H-*meta*-Ph), 7.20 (*dd*, *J* = 7.6, 1H, H-*para*-Ph), 7.11–7.09 (*m*, 1H, H-3-furyl), 5.03 (*s*, 2H, H-7) ppm. ^{13}C {^{1}H} NMR (176.1 MHz, DMSO-d_6, 333 K): δ 164.3, 155.7, 148.1, 139.7, 139.2, 129.8, 128.7 (2C), 124.3, 124.0, 119.5 (2C), 110.0, 106.7, 105.7, 48.8 ppm. IR (KBr), ν (cm^{-1}): 3072, 1686, 1598, 1503, 1452, 1392, 1295, 1266, 1179, 1136, 1035, 878, 754, 690, 606. MS (ESI) *m*/*z*: $[M]^+$ 327 (Br^{79}), 329 (Br^{81}).

Table 3
Experimental details.

Crystal data	
Chemical formula	$C_{16}H_{10}BrNO_2$
M_r	328.16
Crystal system, space group	Orthorhombic, $P2_12_12_1$
Temperature (K)	100
a, *b*, *c* (Å)	4.0229 (5), 12.7225 (16), 24.240 (3)
V (Å^3)	1240.6 (3)
Z	4
Radiation type	Mo $K\alpha$
μ (mm^{-1})	3.31
Crystal size (mm)	0.32 × 0.30 × 0.04
Data collection	
Diffractometer	Bruker Kappa APEXII area-detector
Absorption correction	Multi-scan (*SADABS*; Krause *et al.*, 2015)
T_{min}, T_{max}	0.417, 0.879
No. of measured, independent and observed [$I > 2\sigma(I)$] reflections	18771, 3594, 2973
R_{int}	0.077
(sin $\theta/\lambda)_{max}$ (Å^{-1})	0.703
Refinement	
$R[F^2 > 2\sigma(F^2)]$, $wR(F^2)$, *S*	0.040, 0.078, 1.02
No. of reflections	3594
No. of parameters	181
H-atom treatment	H-atom parameters constrained
$\Delta\rho_{max}$, $\Delta\rho_{min}$ (e Å^{-3})	0.52, −0.62
Absolute structure	Flack *x* determined using 1016 quotients $[(I^+)-(I^-)]/[(I^+)+(I^-)]$ (Parsons *et al.*, 2013)
Absolute structure parameter	0.022 (10)

Computer programs: *APEX2* and *SAINT* (Bruker, 2007), *SHELXS97* (Sheldrick, 2008), *SHELXL2014* (Sheldrick, 2015), *ORTEP-3 for Windows* (Farrugia, 2012) and *PLATON* (Spek, 2020).

6. Refinement

Crystal data, data collection and structure refinement details are summarized in Table 3. All hydrogen atoms were positioned geometrically and refined using a riding model, with C—H = 0.95 and 0.99 Å, and with U_{iso}(H) = 1.2U_{eq}(C). Five reflections (0 1 1, 0 0 2, 0 1 3, 0 1 2 and 0 2 0) affected by the incident beam-stop, as well as nine reflections showing poor agreement between observed and calculated intensities (3 0 26, 0 13 9, 3 0 25, 4 12 5, −3 8 22, 0 11 8, 4 4 18, 0 5 32 and 0 2 26), were omitted in the final cycles of refinement. The remaining positive and negative residual electron densities are both located near the bromine atom (at 1.11 and 0.77 Å, respectively).

Acknowledgements

The authors' contributions are as follows; conceptualization, MA, GMM; synthesis, KAA; X-ray analysis, MSG, IAK; founding, NAM, KIH; writing (review and editing of the manuscript) MA, KIH, RZN; supervision, MA, GMM.

Funding information

Funding for this research was provided by the Russian Science Foundation (project No. 23–43–10024) and the Belarusian Republican Foundation for Fundamental Research (project No. X23RNF-051).

References

Alekseeva, K. A., Fedoseeva, M. A., Bakhanovich, O. V., Khrustalev, V. N., Potkin, V. I., Zhou, H., Nikitina, E. V., Zaytsev, V. P. & Zubkov, F. I. (2024). *J. Org. Chem.* **89**, 3065–3071.

Alekseeva, K. A., Kvyatkovskaya, E. A., Nikitina, E. V., Zaytsev, V. P., Eroshkina, S. M., Shikhaliev, K. S., Truong, H. H., Khrustalev, V. N. & Zubkov, F. I. (2020). *Synlett* **31**, 255–260.

Alekseeva, K. A., Nadirova, M. A., Zaytsev, V. P., Nikitina, E. V., Grigoriev, M. S., Novikov, A. P., Kolesnik, I. A., Mayer, B., Müller, T. J. J. & Zubkov, F. I. (2023). *J. Org. Chem.* **88**, 15029–15040.

Apponyi, M. A., Bowie, J. H., Skelton, B. W. & White, A. H. (2002). *Aust. J. Chem.* **55**, 343–348.

Bernstein, J., Davis, R. E., Shimoni, L. & Chang, N.-L. (1995). *Angew. Chem. Int. Ed. Engl.* **34**, 1555–1573.

Bruker (2007). *APEX2* and *SAINT*. Bruker AXS Inc., Madison, Wisconsin, USA.

Deng, M., Yao, Y., Li, X., Li, N., Zhang, X. & Liang, G. (2019). *Org. Lett.* **21**, 3290–3294.

Farrugia, L. J. (2012). *J. Appl. Cryst.* **45**, 849–854.

Groom, C. R., Bruno, I. J., Lightfoot, M. P. & Ward, S. C. (2016). *Acta Cryst.* B**72**, 171–179.

He, Y., Li, X.-M., Hong, T.-Y. & Yang, J.-K. (2022). *CSD Communication*.

Horak, Y. I., Lytvyn, R. Z., Zubkov, F. I., Nikitina, E. V., Homza, Y. V., Lis, T., Kinzhybalo, V. & Obushak, M. D. (2013). *Acta Cryst.* E**69**, o273–o274.

Krause, L., Herbst-Irmer, R., Sheldrick, G. M. & Stalke, D. (2015). *J. Appl. Cryst.* **48**, 3–10.

Krishna, G., Grudinin, D. G., Nikitina, E. V. & Zubkov, F. I. (2022). *Synthesis* **54**, 797–863.

Ou-Ichen, Z., Boussetta, A., Ouchetto, K., Hafid, A., Khouili, M. & Ouchetto, H. (2024). *J. Iran. Chem. Soc.* **21**, 1453–1493.

Parsons, S., Flack, H. D. & Wagner, T. (2013). *Acta Cryst.* B**69**, 249–259.

Sheldrick, G. M. (2008). *Acta Cryst.* A**64**, 112–122.

Sheldrick, G. M. (2015). *Acta Cryst.* C**71**, 3–8.

Spackman, P. R., Turner, M. J., McKinnon, J. J., Wolff, S. K., Grimwood, D. J., Jayatilaka, D. & Spackman, M. A. (2021). *J. Appl. Cryst.* **54**, 1006–1011.

Speck, K. & Magauer, T. (2013). *Beilstein J. Org. Chem.* **9**, 2048–2078.

Spek, A. L. (2020). *Acta Cryst.* E**76**, 1–11.

Venkatesan, P., Thamotharan, S., Ilangovan, A., Liang, H. & Sundius, T. (2016). *Spectrochim. Acta A Mol. Biomol. Spectrosc.* **153**, 625–636.

Voronov, A. A., Alekseeva, K. A., Ryzhkova, E. A., Zarubaev, V. V., Galochkina, A. V., Zaytsev, V. P., Majik, M. S., Tilve, S. G., Gurbanov, A. V. & Zubkov, F. I. (2018). *Tetrahedron Lett.* **59**, 1108–1111.

Weintraub, R. A. & Wang, X. (2023). *Synthesis* **55**, 519–546.

Zaytsev, V. P., Chervyakova, L. V., Sorokina, E. A., Vasilyev, K. A., Çelikesir, S. T., Akkurt, M. & Bhattarai, A. (2021). *Acta Cryst.* E**77**, 86–90.

Zaytsev, V. P., Lovtsevich, L. V., Pokazeev, K. M., Sorokina, E. A., Dorovatovskii, P. V., Khrustalev, V. N., Romanycheva, A. A., Shetnev, A. A., Volobueva, A. S., Esaulkova, I. L., Slita, A. V., Zarubaev, V. V. & Zubkov, F. I. (2023). *Tetrahedron* **131**, 133205.

Zhou, L., Zhang, M., Li, W. & Zhang, J. (2014). *Angew. Chem. Int. Ed.* **53**, 6542–6545.

Zubkov, F. I., Zaytsev, V. P., Mertsalov, D. F., Nikitina, E. V., Horak, Y. I., Lytvyn, R. Z., Homza, Y. V., Obushak, M. D., Dorovatovskii, P. V., Khrustalev, V. N. & Varlamov, A. V. (2016). *Tetrahedron* **72**, 2239–2253.

supporting information

Acta Cryst. (2025). E**81**, 844-848 [https://doi.org/10.1107/S2056989025007170]

Crystal structure and Hirshfeld surface analysis of 4-bromo-6-phenyl-6,7-dihydro-5*H*-furo[2,3-*f*]isoindol-5-one

Kseniia A. Alekseeva, Mikhail S. Grigoriev, Irina A. Kolesnik, Narmin A. Murshudlu, Khudayar I. Hasanov, Roya Z. Nazarova, Mehmet Akkurt and Gizachew Mulugeta Manahelohe

Computing details

4-Bromo-6-phenyl-6,7-dihydro-5*H*-furo[2,3-*f*]isoindol-5-one

Crystal data

$C_{16}H_{10}BrNO_2$
M_r = 328.16
Orthorhombic, $P2_12_12_1$
a = 4.0229 (5) Å
b = 12.7225 (16) Å
c = 24.240 (3) Å
V = 1240.6 (3) Å^3
Z = 4
$F(000)$ = 656
D_x = 1.757 Mg m^{-3}
Mo $K\alpha$ radiation, λ = 0.71073 Å
Cell parameters from 3489 reflections
θ = 3.0–25.4°
μ = 3.31 mm^{-1}
T = 100 K
Plate, colourless
0.32 × 0.30 × 0.04 mm

Data collection

Bruker Kappa APEXII area-detector diffractometer
φ and ω scans
Absorption correction: multi-scan (SADABS; Krause *et al.*, 2015)
T_{min} = 0.417, T_{max} = 0.879
18771 measured reflections
3594 independent reflections
2973 reflections with $I > 2\sigma(I)$
R_{int} = 0.077
θ_{max} = 30.0°, θ_{min} = 3.3°
h = −5→5
k = −16→17
l = −34→33

Refinement

Refinement on F^2
Least-squares matrix: full
$R[F^2 > 2\sigma(F^2)]$ = 0.040
$wR(F^2)$ = 0.078
S = 1.02
3594 reflections
181 parameters
0 restraints
Hydrogen site location: inferred from neighbouring sites
H-atom parameters constrained
$w = 1/[\sigma^2(F_o^2) + (0.0274P)^2]$ where $P = (F_o^2 + 2F_c^2)/3$
$(\Delta/\sigma)_{max}$ = 0.001
$\Delta\rho_{max}$ = 0.52 e Å^{-3}
$\Delta\rho_{min}$ = −0.62 e Å^{-3}
Absolute structure: Flack x determined using 1016 quotients $[(I^+)-(I^-)]/[(I^+)+(I^-)]$ (Parsons *et al.*, 2013)
Absolute structure parameter: 0.022 (10)

Special details

Geometry. All esds (except the esd in the dihedral angle between two l.s. planes) are estimated using the full covariance matrix. The cell esds are taken into account individually in the estimation of esds in distances, angles and torsion angles; correlations between esds in cell parameters are only used when they are defined by crystal symmetry. An approximate (isotropic) treatment of cell esds is used for estimating esds involving l.s. planes.

Fractional atomic coordinates and isotropic or equivalent isotropic displacement parameters (Å²)

	x	*y*	*z*	U_{iso}*/U_{eq}
C2	0.1419 (11)	0.4353 (3)	0.53657 (19)	0.0205 (10)
H2A	0.039792	0.449845	0.502063	0.025*
C3	0.2950 (10)	0.3444 (3)	0.54847 (16)	0.0200 (8)
H3A	0.320895	0.285576	0.524699	0.024*
C3A	0.4127 (10)	0.3535 (3)	0.60449 (17)	0.0167 (9)
C4	0.5804 (10)	0.2896 (3)	0.64168 (19)	0.0161 (9)
C4A	0.6479 (10)	0.3280 (3)	0.69413 (18)	0.0147 (9)
C5	0.8145 (11)	0.2779 (3)	0.74191 (17)	0.0163 (9)
C7	0.6555 (10)	0.4511 (3)	0.76800 (17)	0.0150 (9)
H7A	0.811196	0.511277	0.769853	0.018*
H7B	0.461702	0.465597	0.791989	0.018*
C7A	0.5487 (10)	0.4299 (3)	0.70951 (19)	0.0155 (9)
C8	0.3782 (11)	0.4975 (3)	0.67421 (19)	0.0188 (10)
H8A	0.311613	0.566361	0.684592	0.023*
C8A	0.3142 (10)	0.4549 (3)	0.62221 (18)	0.0170 (8)
C11	0.9486 (9)	0.3387 (3)	0.83835 (17)	0.0149 (8)
C12	1.1382 (11)	0.2504 (3)	0.8542 (2)	0.0198 (10)
H12A	1.187944	0.197127	0.827962	0.024*
C13	1.2511 (13)	0.2415 (3)	0.90762 (18)	0.0220 (9)
H13A	1.378112	0.181725	0.917973	0.026*
C14	1.1824 (11)	0.3186 (3)	0.94674 (19)	0.0215 (10)
H14A	1.259007	0.311386	0.983614	0.026*
C15	1.0007 (11)	0.4061 (3)	0.9311 (2)	0.0216 (10)
H15A	0.954266	0.459313	0.957452	0.026*
C16	0.8850 (10)	0.4174 (3)	0.87735 (19)	0.0178 (9)
H16A	0.763101	0.478337	0.867127	0.021*
Br1	0.71800 (10)	0.15364 (3)	0.61842 (2)	0.01845 (12)
N6	0.8208 (8)	0.3525 (2)	0.78384 (14)	0.0160 (7)
O1	0.1493 (8)	0.5055 (2)	0.58015 (12)	0.0221 (8)
O2	0.9264 (8)	0.1878 (2)	0.74491 (13)	0.0206 (7)

Atomic displacement parameters (Å²)

	U^{11}	U^{22}	U^{33}	U^{12}	U^{13}	U^{23}
C2	0.020 (2)	0.026 (2)	0.015 (2)	0.0007 (18)	−0.0004 (19)	−0.0008 (18)
C3	0.019 (2)	0.025 (2)	0.016 (2)	−0.004 (2)	0.0013 (18)	−0.0036 (18)
C3A	0.0174 (18)	0.016 (2)	0.017 (2)	−0.0025 (17)	0.0048 (16)	0.0012 (18)
C4	0.015 (2)	0.010 (2)	0.023 (3)	−0.0015 (15)	0.0071 (18)	−0.0017 (17)
C4A	0.0145 (19)	0.010 (2)	0.020 (2)	−0.0007 (14)	0.0036 (16)	0.0018 (15)

C5	0.018 (2)	0.0134 (18)	0.018 (2)	−0.0019 (16)	0.0033 (19)	0.0004 (16)
C7	0.017 (2)	0.0124 (19)	0.016 (2)	0.0004 (15)	0.0021 (18)	0.0000 (16)
C7A	0.016 (2)	0.012 (2)	0.019 (2)	−0.0004 (16)	0.0037 (18)	−0.0009 (17)
C8	0.017 (2)	0.015 (2)	0.024 (3)	0.0031 (16)	0.0043 (18)	−0.0005 (19)
C8A	0.0164 (19)	0.0164 (18)	0.018 (2)	0.0002 (15)	0.000 (2)	0.0032 (17)
C11	0.0139 (19)	0.014 (2)	0.017 (2)	−0.0021 (17)	0.0039 (16)	0.0023 (18)
C12	0.019 (2)	0.014 (2)	0.027 (3)	−0.0009 (16)	0.000 (2)	0.0022 (18)
C13	0.020 (2)	0.0184 (19)	0.027 (2)	−0.002 (2)	−0.001 (2)	0.0050 (17)
C14	0.022 (2)	0.023 (2)	0.020 (2)	−0.0056 (18)	0.001 (2)	0.0036 (17)
C15	0.017 (2)	0.022 (2)	0.026 (3)	−0.0022 (18)	0.005 (2)	−0.005 (2)
C16	0.0175 (19)	0.015 (2)	0.020 (2)	0.0000 (14)	0.000 (2)	−0.0019 (19)
Br1	0.02005 (19)	0.01300 (17)	0.0223 (2)	0.00054 (17)	0.0027 (2)	−0.00368 (18)
N6	0.0195 (17)	0.0117 (15)	0.0168 (17)	−0.0017 (16)	0.0024 (14)	−0.0014 (15)
O1	0.027 (2)	0.0178 (16)	0.0215 (18)	0.0016 (13)	−0.0013 (14)	0.0030 (13)
O2	0.0301 (18)	0.0098 (14)	0.0217 (19)	0.0055 (12)	−0.0003 (14)	0.0004 (12)

Geometric parameters (Å, º)

C2—C3	1.342 (6)	C7A—C8	1.393 (6)
C2—O1	1.384 (5)	C8—C8A	1.396 (6)
C2—H2A	0.9500	C8—H8A	0.9500
C3—C3A	1.443 (5)	C8A—O1	1.376 (5)
C3—H3A	0.9500	C11—C16	1.401 (6)
C3A—C4	1.389 (6)	C11—C12	1.411 (6)
C3A—C8A	1.416 (5)	C11—N6	1.429 (5)
C4—C4A	1.389 (6)	C12—C13	1.378 (6)
C4—Br1	1.902 (4)	C12—H12A	0.9500
C4A—C7A	1.407 (5)	C13—C14	1.392 (6)
C4A—C5	1.482 (6)	C13—H13A	0.9500
C5—O2	1.233 (4)	C14—C15	1.385 (6)
C5—N6	1.391 (5)	C14—H14A	0.9500
C7—N6	1.470 (5)	C15—C16	1.390 (6)
C7—C7A	1.506 (6)	C15—H15A	0.9500
C7—H7A	0.9900	C16—H16A	0.9500
C7—H7B	0.9900		
C3—C2—O1	112.5 (4)	C7A—C8—H8A	123.0
C3—C2—H2A	123.8	C8A—C8—H8A	123.0
O1—C2—H2A	123.8	O1—C8A—C8	125.2 (4)
C2—C3—C3A	106.5 (4)	O1—C8A—C3A	109.7 (4)
C2—C3—H3A	126.8	C8—C8A—C3A	125.2 (4)
C3A—C3—H3A	126.8	C16—C11—C12	119.0 (4)
C4—C3A—C8A	118.2 (4)	C16—C11—N6	118.1 (4)
C4—C3A—C3	136.3 (4)	C12—C11—N6	122.9 (4)
C8A—C3A—C3	105.5 (4)	C13—C12—C11	119.9 (4)
C4A—C4—C3A	118.9 (4)	C13—C12—H12A	120.0
C4A—C4—Br1	122.3 (3)	C11—C12—H12A	120.0
C3A—C4—Br1	118.8 (3)	C12—C13—C14	121.1 (4)

C4—C4A—C7A	120.7 (4)	C12—C13—H13A	119.4
C4—C4A—C5	130.8 (4)	C14—C13—H13A	119.4
C7A—C4A—C5	108.5 (4)	C15—C14—C13	119.0 (4)
O2—C5—N6	125.8 (4)	C15—C14—H14A	120.5
O2—C5—C4A	127.6 (4)	C13—C14—H14A	120.5
N6—C5—C4A	106.6 (3)	C14—C15—C16	121.1 (4)
N6—C7—C7A	102.8 (3)	C14—C15—H15A	119.4
N6—C7—H7A	111.2	C16—C15—H15A	119.4
C7A—C7—H7A	111.2	C15—C16—C11	119.8 (4)
N6—C7—H7B	111.2	C15—C16—H16A	120.1
C7A—C7—H7B	111.2	C11—C16—H16A	120.1
H7A—C7—H7B	109.1	C5—N6—C11	126.7 (3)
C8—C7A—C4A	123.1 (4)	C5—N6—C7	112.5 (3)
C8—C7A—C7	127.5 (4)	C11—N6—C7	120.6 (3)
C4A—C7A—C7	109.5 (4)	C8A—O1—C2	105.9 (3)
C7A—C8—C8A	113.9 (4)		

O1—C2—C3—C3A	0.5 (5)	C4—C3A—C8A—O1	−179.3 (3)
C2—C3—C3A—C4	178.6 (5)	C3—C3A—C8A—O1	−0.4 (4)
C2—C3—C3A—C8A	0.0 (4)	C4—C3A—C8A—C8	1.4 (6)
C8A—C3A—C4—C4A	−0.8 (6)	C3—C3A—C8A—C8	−179.7 (4)
C3—C3A—C4—C4A	−179.3 (4)	C16—C11—C12—C13	1.5 (6)
C8A—C3A—C4—Br1	−179.5 (3)	N6—C11—C12—C13	−179.4 (4)
C3—C3A—C4—Br1	2.1 (7)	C11—C12—C13—C14	−0.2 (7)
C3A—C4—C4A—C7A	−0.1 (6)	C12—C13—C14—C15	−0.8 (7)
Br1—C4—C4A—C7A	178.6 (3)	C13—C14—C15—C16	0.5 (7)
C3A—C4—C4A—C5	178.8 (4)	C14—C15—C16—C11	0.8 (6)
Br1—C4—C4A—C5	−2.6 (6)	C12—C11—C16—C15	−1.8 (6)
C4—C4A—C5—O2	−1.2 (8)	N6—C11—C16—C15	179.0 (4)
C7A—C4A—C5—O2	177.7 (4)	O2—C5—N6—C11	−1.8 (7)
C4—C4A—C5—N6	179.0 (4)	C4A—C5—N6—C11	178.0 (3)
C7A—C4A—C5—N6	−2.1 (5)	O2—C5—N6—C7	−177.8 (4)
C4—C4A—C7A—C8	0.4 (6)	C4A—C5—N6—C7	2.0 (5)
C5—C4A—C7A—C8	−178.6 (4)	C16—C11—N6—C5	−170.0 (4)
C4—C4A—C7A—C7	−179.5 (4)	C12—C11—N6—C5	10.9 (6)
C5—C4A—C7A—C7	1.4 (5)	C16—C11—N6—C7	5.7 (5)
N6—C7—C7A—C8	179.8 (4)	C12—C11—N6—C7	−173.4 (4)
N6—C7—C7A—C4A	−0.2 (4)	C7A—C7—N6—C5	−1.2 (4)
C4A—C7A—C8—C8A	0.1 (6)	C7A—C7—N6—C11	−177.4 (3)
C7—C7A—C8—C8A	−179.9 (4)	C8—C8A—O1—C2	179.9 (4)
C7A—C8—C8A—O1	179.8 (4)	C3A—C8A—O1—C2	0.7 (4)
C7A—C8—C8A—C3A	−1.0 (6)	C3—C2—O1—C8A	−0.7 (5)

Hydrogen-bond geometry (Å, º)

D—H···*A*	*D*—H	H···*A*	*D*···*A*	*D*—H···*A*
C7—H7*A*···O2^{i}	0.99	2.51	3.463 (5)	162
C8—H8*A*···O2^{ii}	0.95	2.49	3.348 (5)	149

C12—H12*A*···O2	0.95	2.27	2.894 (6)	122
C16—H16*A*···Br1^{ii}	0.95	2.97	3.864 (4)	157

Symmetry codes: (i) −*x*+2, *y*+1/2, −*z*+3/2; (ii) −*x*+1, *y*+1/2, −*z*+3/2.